Contents lists available at SciOpen

Food Science and Human Wellness

journal homepage: https://www.sciopen.com/journal/2097-0765

China Food Publishing Co.

A gut-brain connection: probiotics L9 and A6 offer new insights into Alzheimer's disease prevention

Zhe Sun[a,1], Bing Fang[a,1], Haina Gao[a], Yuhang Sun[a], Yue Liu[a], Huiyuan Guo[b], Liang Zhao[c,d], Fazheng Ren[b], Ming Zhang[a,*]

[a] School of Food and Health, Beijing Technology and Business University, Beijing 100048, China
[b] Key Laboratory of Precision Nutrition and Food Quality, Department of Nutrition and Health, China Agricultural University, Beijing 100083 China
[c] Key Laboratory of Functional Dairy, College of Food Science and Nutritional Engineering, China Agricultural University, Beijing 100083, China
[d] Beijing Laboratory of Food Quality and Safety, College of Food Science and Nutritional Engineering, China Agricultural University, Beijing 100083, China

ARTICLE INFO

Article history:
Received 3 November 2023
Received in revised form 13 March 2024
Accepted 1 July 2024

Keywords:
Lacticaseibacillus paracasei
Bifidobacterium animalis subsp. *lactis*
Alzheimer's disease
Gut microbiome
Serum metabolomics

ABSTRACT

Accumulating evidence suggests that probiotics affect the microbial-gut-brain axis in a way that can prevent and treat Alzheimer's disease (AD). However, the mechanism underlying the therapeutic effects still needs to be further investigated. This study aimed to examine the alleviating effect of *Lacticaseibacillus paracasei* L9 and *Bifidobacterium animalis* subsp. *lactis* A6 and possible mechanism in mice with AD. In this study, the administration of probiotics L9 and A6 effectively improved memory and learning functions in AD mice. The hippocampal cells of mice were partly recovered in morphology and rearranged more neatly after probiotics intervention. Meanwhile, L9 and A6 exhibited inhibitory effects on the phosphorylation of Tau and the deposition of Aβ, which were mediated *via* GSK-3β and PP2A kinases. Meanwhile, by metagenomic sequencing, we found interventions with L9 and A6 altered the intestinal microbiome's taxonomic composition, reduced the abundance of pathogenic *Desulfovibrio* genera, and increased beneficial *Clostridium* and *Paramuribaculum* genera abundance. The fatty acids metabolism and biosynthesis of gut microbiome were also enhanced. Serum untargeted metabolomics also showed noticeable alternation in lipid-related metabolites, which may alleviate the pathogenesis of AD. These results revealed a mitigating role for probiotic L9 and A6 in AD prevention and offer new insights into AD prevention *via* gut-brain connection.

1. Introduction

As the most common neurodegenerative disease, Alzheimer's disease (AD) has become a global health concern[1]. According to relative epidemiology survey, the number of people suffering from dementia worldwide exceeds 50 million, of which the AD may contribute 50%–70% of cases[2]. The primary pathological characteristics of AD are gradual cognitive impairment, the pathological manifestations such as β-amyloid (Aβ) deposits leading to development of senile plaques, and neurofibrillary tangles (NFTs)[3-4]. Hyperphosphorylated Tau protein is the major component of NFTs, disrupting the transport of neurotransmitters and eventually leading to the apoptosis of nerve cells[5]. Multiple protein kinases and phosphatases regulate Tau phosphorylation, such as protein phosphate 2A (PP2A) and glycogen synthase kinase-3β (GSK-3β)[6]. PP2A not only dephosphorylates Tau but also controls the activity of Tau kinases. Therefore, regulating the activity of PP2A may affect the

[1] These authors contributed equally to this work.
[*] Corresponding author at: School of Food and Health, Beijing Technology and Business University, Beijing 100048, China.
E-mail address: zhangming@th.btbu.edu.cn (M. Zhang)
Peer review under responsibility of Beijing Academy of Food Sciences.

SciOpen Publishing services by Tsinghua University Press

http://doi.org/10.26599/FSHW.2024.9250340

occurrence of AD[7]. On the contrary, GSK-3β promotes abnormal Tau hyperphosphorylation inducing destruction of related neuronal structure, promoting the occurrence of AD[8]. In addition, the deposition of Aβ is also a key factor affecting the phosphorylation of Tau protein and causes changes in the expression of relevant inflammatory factors[9]. Therefore, deposition of Aβ and hyperphosphorylated Tau protein were generally regarded as the prevention and therapeutic targets of AD.

Regulating the disturbed gut-brain axis may have great potential in the treatment of central nervous system diseases[10], which is a bidirectional system of regulation connected to the nervous, immune, and metabolic systems of the gut and brain[11]. Gut microbiota dysbiosis is prevalent in AD patients and model animals, in which the Firmicutes abundance was decreased but the abundances of Bacteroidetes and Proteobacteria were increased[12]. The dysbiosis microbiota is prone to enhance systemic inflammation and then the occurrence of neurodegenerative diseases. A previous study demonstrated that *Escherichia* and *Shigella* were more abundant in patients with cognitively impaired and amyloid-positive, and showed positive correlations with inflammatory response[13]. Another pro-inflammatory species *Helicobacter pylori* also induced Alzheimer-like Tau hyperphosphorylation through the activation of GSK-3β[14-15]. However, clinical evidence found that the relative abundances of *Eubacterium rectale* and *Bacteriodes fragilis* with the anti-inflammatory function were reduced in cognition-impaired elderly patients[16]. Similarly, a clinical study have found that the abundance of some anti-inflammatory bacteria that can produce butyric acid was significantly reduced in AD patients, such as *Clostridium* cluster IV genus and *Butyricicoccus*[17]. Therefore, the intervention of intestinal flora may reduce the inflammatory response and damage of hippocampal tissue to relieve the AD-related symptoms.

Probiotics, as a potential therapeutic strategy, can affect the central nervous system to prevent or improve AD symptoms[18]. Numerous studies have shown that probiotics have significant remission effects in AD models. For example, the cognitive function of AD mice was improved and the Aβ-induced inflammatory response was inhibited after the oral administration of *Bifidobacterium brevis* A1[19]. *Lactobacillus plantarum* DP189 could prevent AD by regulating intestinal flora and the PI3K/Akt/GSK-3β pathway[20]. *Bifidobacterium breve* MCC1274 could reduce neuroinflammation and inhibit Tau phosphorylation, thus reducing AD-like pathologies in wild-type mice[21]. *Bifidobacterium longum* NK46 mitigated the reduction in cognitive function by regulating LPS-induced activation of NF-κB and inhibiting intestinal microbial dysregulation[22]. However, detailed changes happened to intestinal microbiome, as an important target for probiotic intervention in the above studies, was not clarified. Whether the alterations of gut microbiota contribute to changes in immune and metabolic pathways of the gut-brain connection still needs further investigation.

Lacticaseibacillus paracasei L9 (L9) is a probiotic that enhanced immune regulation and inflammation response in the body[23]. Another study showed that *Bifidobacterium animalis* subsp. *lactis* A6 (A6) was highly acid-tolerated and attenuated DSS-induced colitis by inhibiting excessive proinflammatory response[24-25]. The objective of this study is to investigate the impact of L9 and A6 on the cognitive abilities of mice with AD. In order to validate the potential modifying effects of probiotics, metagenomic sequencing and untargeted metabolomics techniques were employed to examine the specific changes in gut microbiota and serum metabolome that contribute to the alleviation of AD symptoms.

2. Materials and methods

2.1 Probiotic cells

L9 and A6 were provided by the Department of Nutrition and Health of China Agricultural University. For the collection of bacterial cells, L9 and A6 were grown in MRS broth overnight at 37 ℃, collected by centrifugation, and counted by serial dilutions.

2.2 Animals and treatments

Experimental Animal Ethics and Welfare Committee of China Agricultural University approved and guided the experiment (AW31903202-5-2). A total of 40 SPF male BALB/c mice (5 weeks) were obtained from Huafukang Biotechnology Co., Ltd. (Beijing, China). After 1 week of adaption, using a random number generator, the mice were divided into 4 groups of 10 each, as follows: Group 1, untreated control group (Control); Group 2, mice treated with $AlCl_3$ and *D*-gal (AD model); Group 3, L9 (5×10^{11} CFU/mL, 0.2 mL) treated during $AlCl_3$ and *D*-gal administration (L9); Group 4, A6 (5×10^{11} CFU/mL, 0.2 mL) treated during $AlCl_3$ and *D*-gal administration (A6). Mice in AD, L9, and A6 groups were received 0.1 mL $AlCl_3$ (4 mg/mL) by gavage and subcutaneous injection of 0.1 mL *D*-gal (24 mg/mL) daily for 8 weeks. All the mice were anesthetized to collect blood by eyeball extirpating after behavioral tests. The serum was acquired by the centrifugation. Following the sacrifice of the mice, tissue samples were collected and stored at –80 ℃ for subsequent detection.

2.3 Behavioral tests

Morris water maze (MWM) and step-down type passive avoidance (Step-down) tests were performed in a blinded manner to assess the different cognitive capacities of mice in this study. The MWM test is a widely used experimental paradigm for assessing spatial memory in mice that relies on the hippocampus. As previously described[26], this study used a circular water maze with a 120 cm diameter and a 40 cm height, and 25 ℃ temperature. As an escape point, a circular platform with a diameter of 2 cm was positioned 2 cm below the water's surface. The experimental protocol consisted of a 4-day training phase, during which the mice were trained to locate the escape platform. We conducted a probe test on day 5 by taking out the platform and placing the mice in water, replicated the previous training session.

As previously described[27], the step-down test comprised eight individual paralleled plastic boxes (Zhenghua Biological Instrument Equipment Co., Ltd., Huaibei, China). A training session followed by a retention session were included in whole test protocol. Each mouse was introduced to the box and allowed 3 min to adapt during the training session. Subsequently, the mouse was positioned on the steel grids and subjected to an electric shock of 0.35 mA for a duration of 5 min. In response to the electric shock, the mice escaped from the grid floor and returned to the platform. After 24-h training, mice were placed on the platform and measured step-down latency (time taken for the first step from platform to grid floor) and error rate.

2.4 Haematoxylin and eosin (HE) staining

All the mice were sacrificed after blood sampling, 5 mice were selected at random for the following cardiac perfusion in each group. Fresh hippocampi and cerebral cortex were then dissected from brains and then embedded in paraffin. The embedded sections were cut for HE staining.

2.5 Western blot (WB) analysis

In addition to the 5 mice for HE section, the hippocampus tissues of remaining mice were used for protein and RNA extraction. To determine protein level expression of typical biomarkers in the hippocampus, WB analysis was performed using primary antibodies against Tau (1:1 000, #TDY640C, TDY Biotech, Beijing, China), phospho-Tau (Ser396, 1:1 000, #9632S, CST, Danvers, USA), phospho-Tau (Ser404, 1:1 000, #20194S, CST, Danvers, USA), $A\beta_{1\text{-}40}$ (1:1 000, #44136, Thermo Fisher Scientific, USA), $A\beta_{1\text{-}42}$ (1:1 000, #AB5078P, Sigma-Aldrich, St. Louis, USA), and β-actin (1:5 000, #bs0061R, Bioss, Beijing, China). A gray value analysis was performed using the ImageJ software.

2.6 Quantitative real-time PCR (qRT-PCR) analysis

Transcribing cDNA from total RNA extracted from hippocampus tissues was performed using the TRNzol reagent (Tiangen Biotechnology, Beijing, China). The primer sequences were synthesized by Invitrogen (Beijing, China) and listed in Table 1. QRT-PCR was performed using the SYBR Green real-time PCR kits (Takara, Dalian, China). Two-step amplification was performed, and the PCR conditions were as follows: predenaturation at 95 ℃ for 30 s, 1 cycle; denatured at 95 ℃ for 5 s, annealed at 60 ℃ for 30 s, 40 cycles. The expressions of mRNA were quantified by the $2^{-\Delta\Delta Ct}$ method and all quantifications were normalized with β-actin.

Table 1
Primer sequences and product sizes.

Primers	Forward/reverse	Primer sequences (5′ to 3′)	Product size (bp)
GSK-3β	Forward	CTCTTGTGGTAGAAACGGAA	123
	Reverse	ATAACCCTGTGAAACTGACC	
PP2A	Forward	AGTTTGACCCAGCACCTC	205
	Reverse	GCACATCTTTTGGTCCGT	
β-Actin	Forward	CGTTGACATCCGTAAAGACCTC	159
	Reverse	ACAGAGTACTTGCGCTCAGGAG	

2.7 Fecal metagenome sequencing

Feces were collected before the mice were sacrificed. Total microbial DNA from fecal samples was extracted by the commercial kit (Omega Biotek, Norcross, GA, USA). The concentrations and quality of DNA were checked with the NanoDrop2000 (Thermo Fisher Scientific, Waltham, MA, USA) and agarose electrophoresis, respectively. Library construction, quality control, genome assembly, gene taxonomic, and functional annotation were performed as previously described[28]. NovaSeq platform (Illumina Inc., San Diego, CA, USA) was used to construct the libraries and sequence them. Subsequently, the raw data were assembled, annotated. Functional metagenomes annotated as Kyoto Encyclopedia of Genes and Genomes (KEGG) Orthologues (KOs) were analyzed using PICRUSt2. The Circos diagram was plotted to describe species or KOs gene abundance and generated by Circos-0.67-7 software. Comparison analysis was determined by principal co-ordinates analysis (PCoA), Wilcoxon rank sum test and linear discriminant analysis (LDA) and generated by Majorbio cloud platform (https://cloud.majorbio.com). All obtained raw sequence datasets have been uploaded to the NCBI Sequence Read Archive (SRA) with the accession number PRJNA1101118.

2.8 Untargeted metabolomics analysis of peripheral serum

Serum samples were analyzed using the LC-mass spectrometry-based untargeted metabolomics. A total of 400 μL methanol-water (1:4, *V*/*V*) was added to each 100 μL serum sample. CentriVap Concentrators (Labconco, MO) were used to dry the supernatant after vortexing and centrifuging. Subsequently, samples were analyzed by mass spectrometry using methods previously described[29]. The brief description is as follows. An Agilent 1290 II UPLC system was used for untargeted metabolomics analysis. For positive mode, C_8 UPLC column (2.1 mm × 100 mm, 1.7 μm) was applied to separate the metabolites at 50 ℃. In the mobile phase A, formic acid was dissolved in water at a rate of 0.1% and in the mobile phase B, formic acid was dissolved in acetonitrile at a rate of 0.1%. A linear gradient elution program was as follows: 0 min, 10% B, 1 min; 5 min, 40% B; 17 min, 100% B, 5 min; decreasing to 10% B within 0.1 min and holding 2.9 min. For negative mode, HSS T3 (2.1 mm × 100 mm, 1.8 μm) column was applied at 50 ℃. Mobile phases C and D were composed of 6.5 mmol/L NH_4HCO_3 in water and methanol/water (95:5, *V*/*V*). A linear gradient elution program was as follows: 0 min, 0% C, 1 min; 3 min, 40% B; 16 min, 100% D, keeping 6 min; decreasing to 0% D within 0.1 min, holding on 2.9 min. The MS scan range was *m*/*z* 50–1 200. The generated raw data were further processed by Agilent Profinder (version 10.0, Agilent Technologies) for peak detection and peak alignment. Mass Profiler Professional Software (version 14.5, Agilent Technologies) was used for normalization and annotation. Metabolites were filtered based on previously criteria[29]. The public metabolism databases including HMDB (https://hmdb.ca) and METLIN (https://metlin.scripps.edu) were used to annotate the metabolites information. Based on the relative quantification of metabolites, comparison analysis was accessed by circos diagram, PCoA, Wilcoxon rank sum test, volcano diagrams, Heatmap diagram which were generated by Majorbio cloud platform (https://cloud.majorbio.com).

2.9 Statistical analysis

All the experimental data were expressed as mean ± standard error mean (SEM). GraphPad Prism 7 software was used for statistical analysis and plotting. ANOVA and Fisher's exact probability test were used to calculate statistical significance. $P < 0.05$ was considered significant. The Spearman's correlation coefficient between different serum metabolites and genus-level intestinal flora was accessed by R (pheatmap package, v. 3.3.1), which was visualized as the heatmap chart.

3. Results

3.1 L9 and A6 treatment ameliorated AD-induced cognitive deficits

To investigate whether L9 and A6 can alleviate learning and memory deficits in AD mice, spatial memory and learning memory were examined by MWM and step-down passive avoidance test. The procedures and treatments of the trial were shown in the Fig. 1A. The typical trajectories for the MWM test were presented in Fig. 1B. The platform crossing times of mice in the AD model group were significantly less than those in the control group ($P < 0.05$). The L9 and A6 intervention significantly increased times of platform-crossing times compared to the AD model group ($P < 0.05$, Fig. 1C). Similarly, compared with the AD model group, L9 and A6 intervention obviously reduced the residence time and movement distance in the target quadrant of mice ($P < 0.05$, Fig. 1C).

A step-down test was used in this study to examine passive avoidance memory of mice, in which the mice with the memory deficit tend to show increased error numbers. In Fig. 1D, the average error number of AD model group was higher than that in control group. However, the mice of L9 and A6 groups both showed fewer error numbers compared to the AD model group, especially in L9 group ($P < 0.05$, Fig. 1D). These results suggested that probiotics A6 and L9 significantly improved learning and memory function in AD mice.

3.2 L9 and A6 treatment alleviated morphological damages of hippocampus

Learning and memory functions were closely correlated with the hippocampal neurons. To observe the morphological change of the hippocampus after intervention of L9 and A6, the HE staining was employed in this study. As shown in Fig. 2A, the cell morphology of hippocampal CA1 region in mice of AD model group was not orderly, and the nucleus showed obvious pyknosis, dissolution, and disappearance. After the intervention with probiotics, hippocampal cells were compact and neatly arranged, the cell morphology in hippocampus CA1 region was clearly improved.

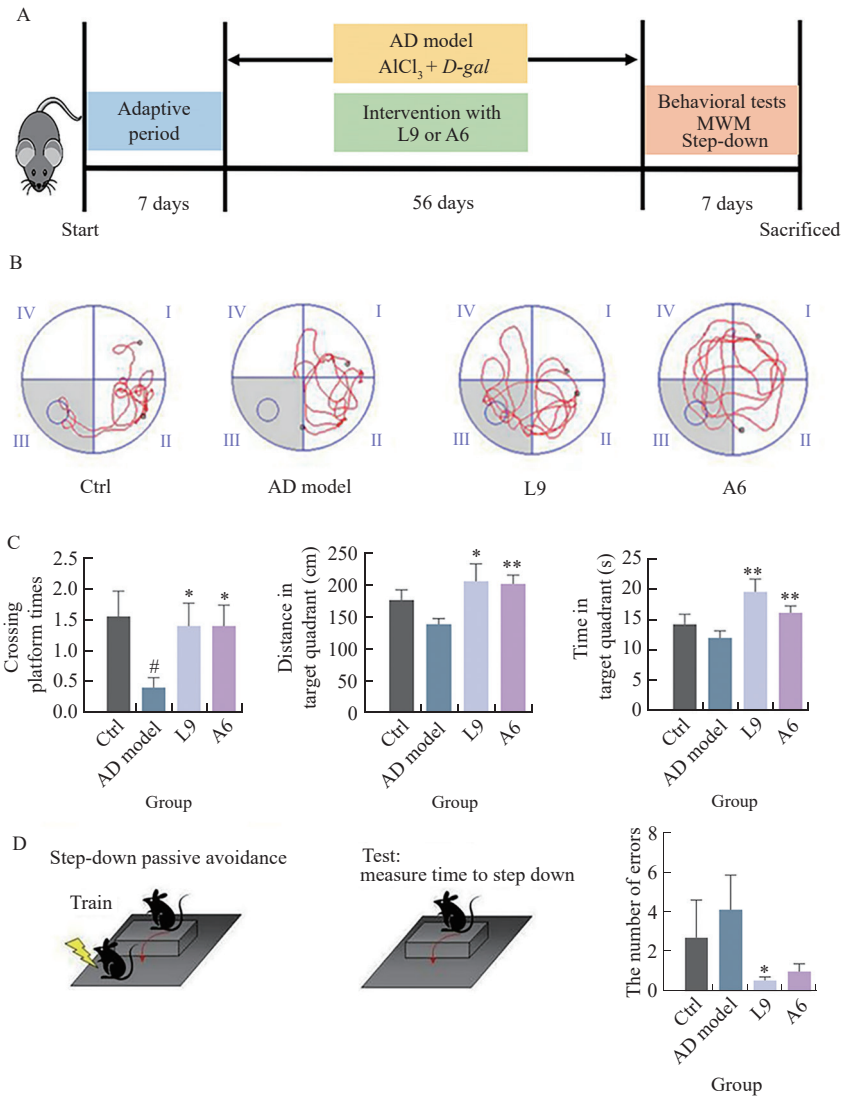

Fig. 1 Effects of L9 and A6 on learning and memory abilities in *D*-gal/$AlCl_3$-induced AD model mice ($n = 10$/group). (A) Study design and animal treatments. (B) Typical MWM trajectories. (C) Platform-crossing times, targeted quadrant distance and time. (D) Graphical representation of step-down test and the number of errors. $^{*}P < 0.05$, $^{**}P < 0.01$ compared to the model group. $^{\#}P < 0.05$ compared to the control group.

The increase in eosinophils in the hippocampus could easily cause tissue damage and promote inflammation. Eosinophils in hippocampus were counted after HE staining, and the results were shown in Fig. 2B. Compared to the AD group, L9 and A6 groups had significantly lower proportions of eosinophils in CA1 of the hippocampus ($P < 0.01$).

3.3 L9 and A6 treatment inhibited the protein expressions of Tau and Aβ in the hippocampus

Aβ plaque deposition and hyperphosphorylated Tau proteins are the major neuropathological features of AD. To investigate the protective role of probiotics against AD pathology, the protein expressions of Tau and Aβ in the hippocampus were detected by WB. Relative to the AD model group, the expression level of total Tau in A6 group was remarkably declined ($P < 0.05$, Fig. 3A). Meanwhile, the relative expression levels of phospho-Tau (Ser396) and phospho-Tau (Ser404) were markedly downregulated in L9 and A6 groups compared to the AD model group ($P < 0.05$, Fig. 3A). Furthermore, the expression of $A\beta_{1\text{-}40}$ or $A\beta_{1\text{-}42}$ in the hippocampus of L9 or A6 group was also suppressed after L9 and A6 intervention ($P < 0.05$, Fig. 3B).

3.4 L9 and A6 treatment modulated the expression of GSK-3β and PP2A mRNA in hippocampus

Given that the phosphorylation of Tau is closely associated with GSK-3β and PP2A, we detected the mRNA expression levels of *GSK-3β* and *PP2A* in hippocampus. As shown in Fig. 3C, the mRNA expression level of *GSK-3β* in hippocampus of AD model

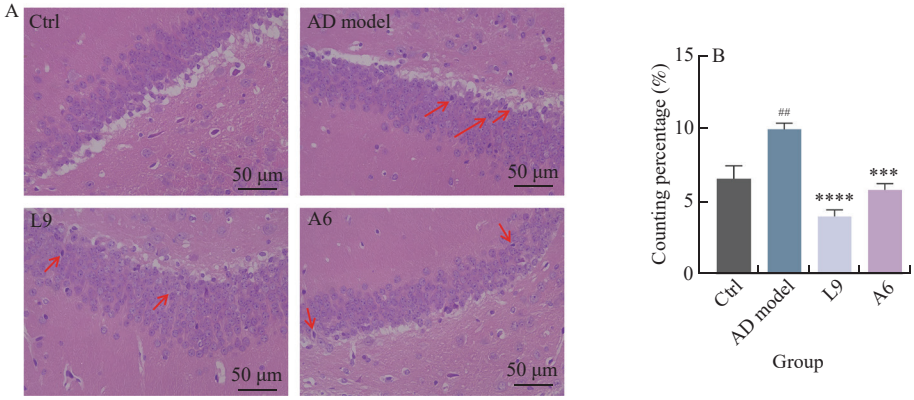

Fig. 2 Ameliorative effects of L9 and A6 on *D*-gal/$AlCl_3$-caused damage of hippocampal neurons in mice. (A) H&E staining of hippocampal CA1 region (40×). (B) Percentage of eosinophils in the CA1 region of the hippocampus of mice. $^{\#\#}P < 0.01$ *vs*. control group; $^{***}P < 0.001$, $^{****}P < 0.000\ 1$ *vs*. model group.

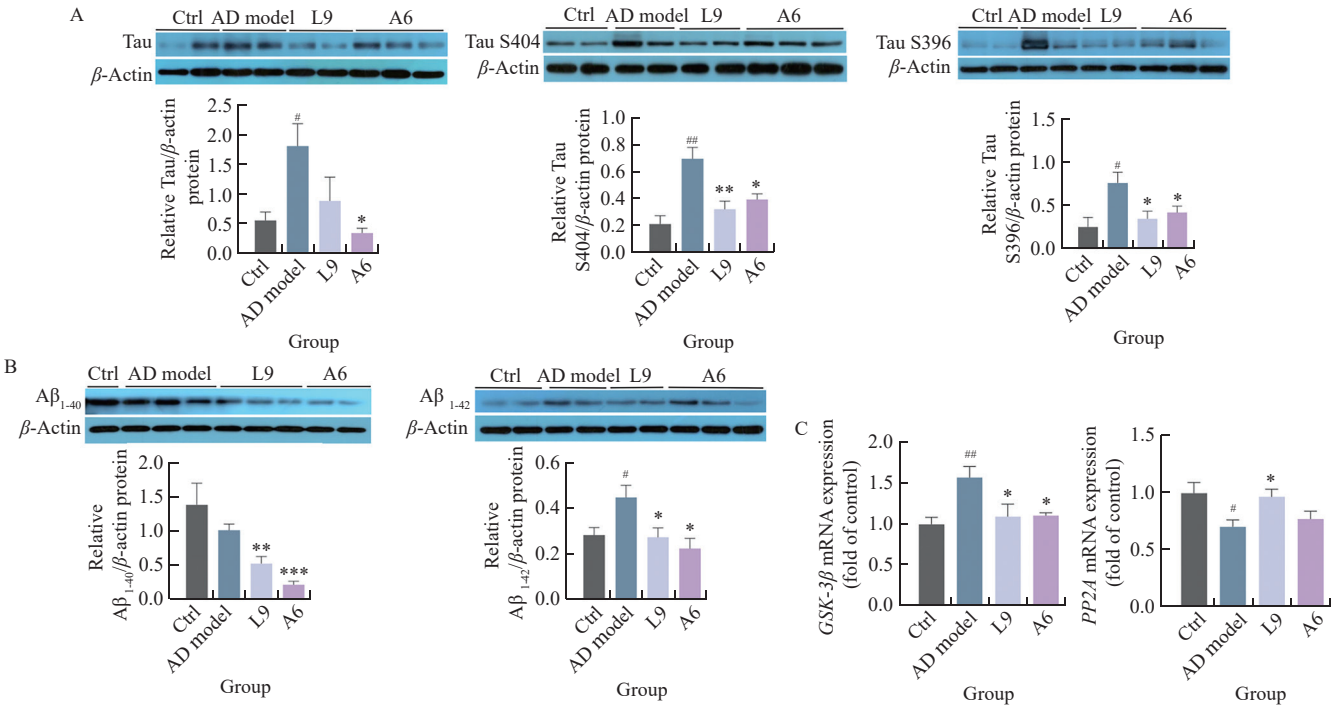

Fig. 3 Effects of L9 and A6 on the protein expressions of Tau and Aβ in the hippocampus and expression of Tau protein phosphorylation-related kinases. (A) Expression level of Tau, Tau S404 and Tau S396. (B) Expression level of $A\beta_{1\text{-}40}$ and $A\beta_{1\text{-}42}$. (C) Relative expression of *GSK-β* and *PP2A* in the hippocampus as determined by RT-PCR. $^{\#}P < 0.05$, $^{\#\#}P < 0.01$ *vs*. control group; $^{*}P < 0.05$; $^{**}P < 0.01$ and $^{***}P < 0.001$ *vs*. model group.

group was higher than that of control group. Compared with the AD model group, *GSK-3β* expressions significantly declined after L9 and A6 interventions ($P < 0.05$). The expression of *PP2A*, on the other hand, was remarkably decreased during the pathogenesis of AD ($P < 0.05$). However, after gavage of L9, the expression of *PP2A* in the hippocampus was markedly elevated ($P < 0.05$).

3.5 L9 and A6 treatment altered the taxonomic composition of intestinal microbiota

To identify the of taxonomic composition alternations of intestinal microbiota, we executed metagenomic gene sequencing. First, the *α*-diversity analysis of microbial community was performed, including Chao index, Simpson index and Shannon index (Fig. S1). There was no significant difference in Chao index between the control and AD model groups, indicating that the richness of gut microbiota in AD mice was not changed (Fig. S1A). The Chao index was significantly higher than that in AD model group after L9 treatment, while there was no significant difference in the Chao index between A6 group and AD model group. Compared with the Control group, AD model group showed an increasing trend in Simpson index, but no statistical difference (Fig. S1B). The Shannon index in AD model group significantly reduced, indicating a change in the diversity of the gut microbiota in AD mice (Fig. S1C). Although there was no significant difference compared to AD model group after L9 intervention, L9 to some extent reduced the Simpson index and increased the Shannon index, suggesting that L9 had a certain improvement effect on the diversity of microbial community. A6 exhibited a similar intervention effect to probiotic L9, but overall it had minimal impact on richness and diversity. The relative abundances of communities were compared and shown in Fig. 4A. Based on genus level, the dominant flora of mice in each group was Muribaculaceae and followed by *Bacteria*, *Lachnospira*, Bacteroidetes and *Prevotella*. *β*-Diversity reflected by the PCoA was performed among the 4 groups and found that there was a noteworthy structural shift along the direction of PC2 between control and AD model group (Fig. 4B). By contrast, after the probiotic L9 and A6 intervention, the structure of the intestinal flora was closer to that of the control group.

To identify taxonomic changes between groups, Wilcoxon rank-sum tests were performed. The probiotics L9 group showed remarkably higher *Clostridium* and *Paramuribaculum* abundance, less *Bacteroides* and *Desulfovibrio* abundance than the AD model group (Fig. 5A, $P < 0.05$). Similarly, the abundance of *Paramuribaculum* was significantly elevated in A6 administrated mice, while the abundance of *Oscillibacter*, *Desulfovibrio*, *Mucispirillum* and *Flavonifractor* were distinctly attenuated after the administration of A6.

Linear discriminant analysis effect size (LEfSe) analysis was then carried out to evaluate the different characteristic taxa among the groups (Fig. 5B). The results based on an LDA score ≥ 3 demonstrated that *Bacteroides*, *Oscillibacter*, and *Desulfovibrio* were discriminative for the AD group; *Clostridium*, *Duncaniella*, *Eubacterium* and *Mucispirillum* were discriminative for the L9 group; *Paramuribaculum* were the only genera discriminative for the A6 group.

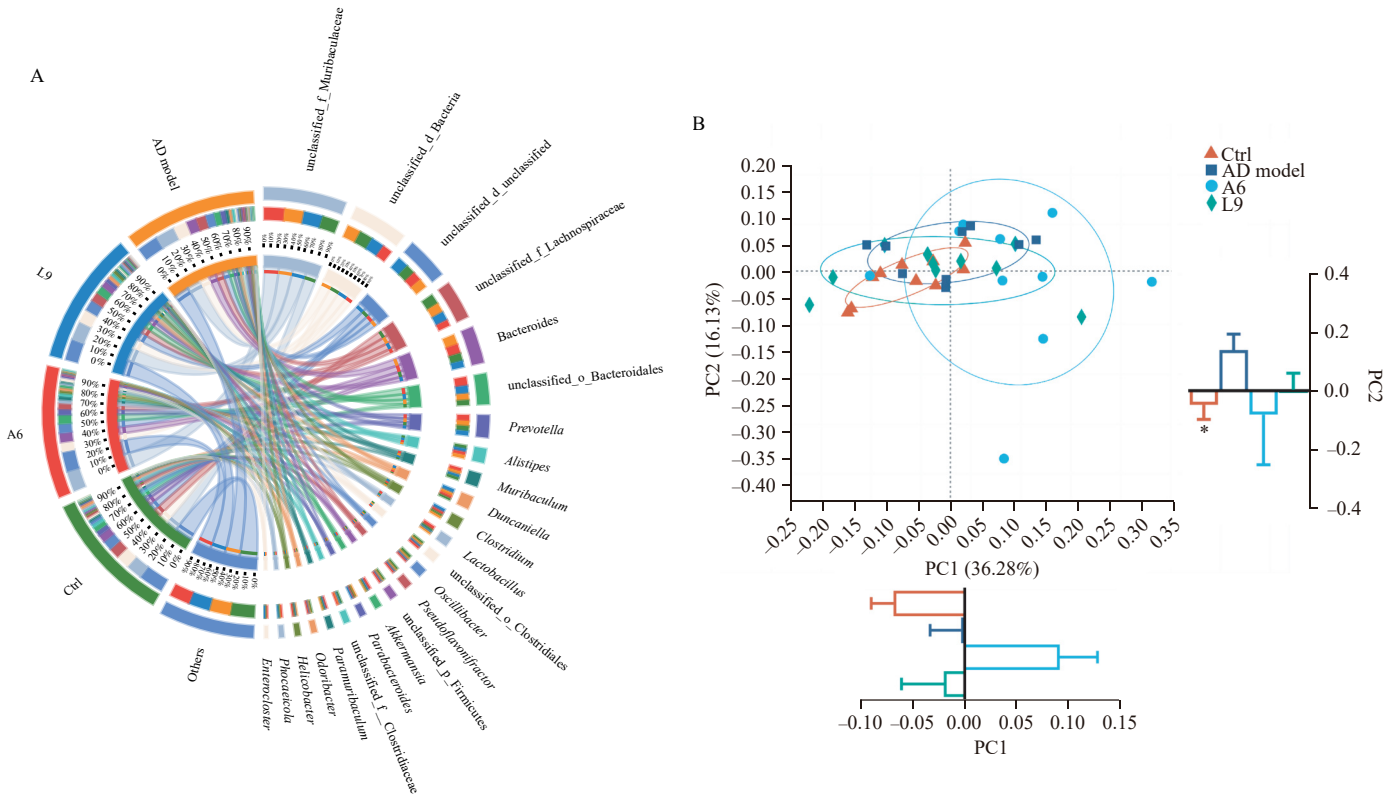

Fig. 4 Taxonomic compositional changes to the gut microbiome after L9 or A6 treatment ($n = 10$/group). (A) Circos diagram shows the taxonomic composition and the correspondences between samples and taxa of different groups at the genus level. (B) PCoA of different groups ($R = 0.142$, $P = 0.001$). *$P < 0.05$ compared to the model group.

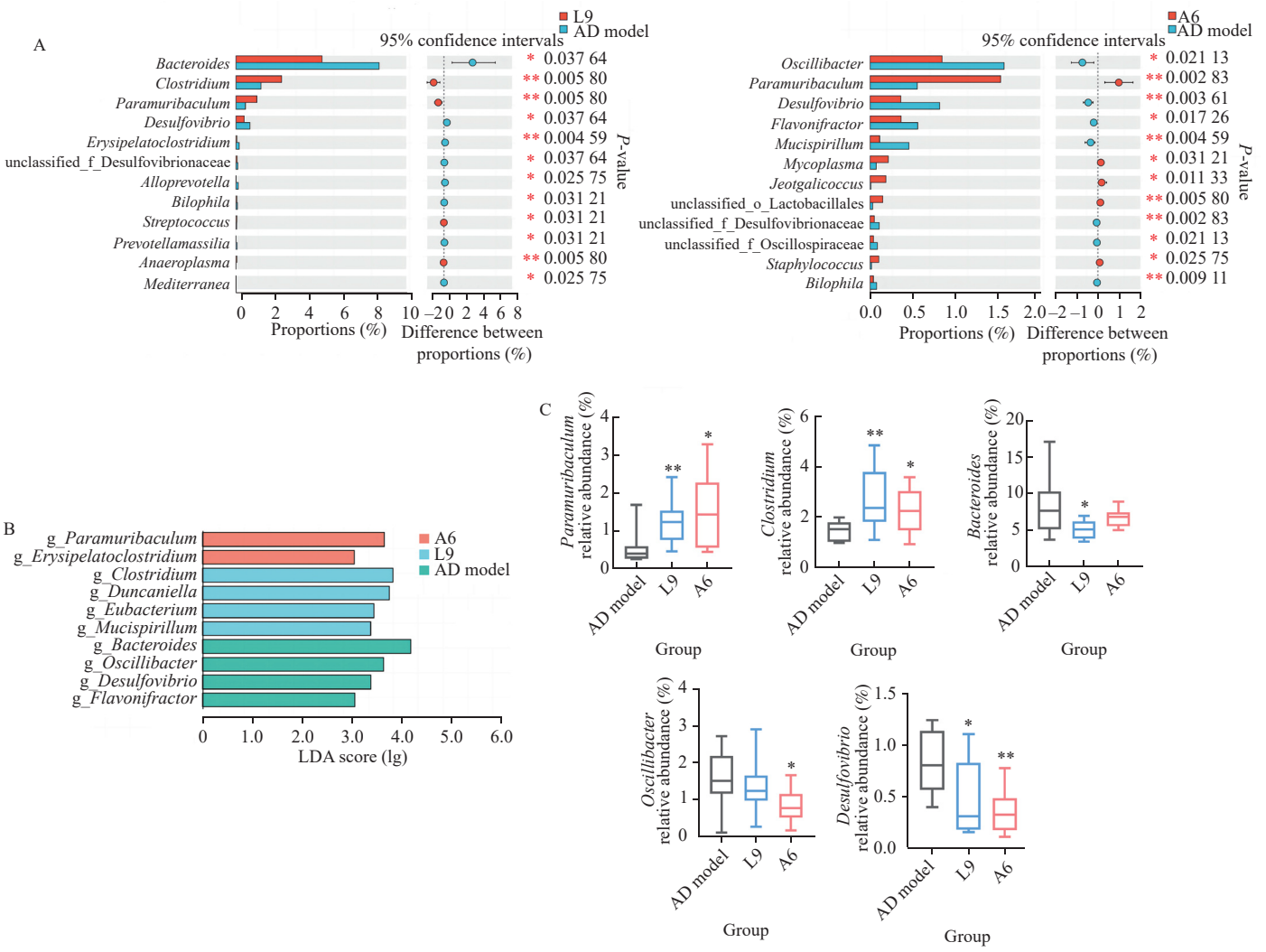

Fig. 5 Effects of L9 or A6 treatment on abundance changes in characteristic taxa at the genus level (n = 10/group). (A) Difference comparisons of species abundances between L9/A6 and AD model groups using the Wilcoxon rank-sum test. (B) LEfSe cladogram represents the significantly changed bacteria associated with different treatments at the genus level (LDAs ≥ 3). (C) Characteristic taxa at the genus level derived from LEfSe analysis. *P < 0.05; **P < 0.01 *vs*. model group.

Following the LEfSe analysis above, differences in characteristic taxa were further analyzed. As shown in Fig. 5C, the abundance of *Clostridium* and *Paramuribaculum* was distinctly enriched after L9 and A6 intervention. By contrast, L9 and A6 groups had significantly lower *Desulfovibrio* abundances (P < 0.05).

3.6 L9 and A6 treatment altered metabolic functions of intestinal microbiota

Utilizing KEGG analysis, this study examined the variations in microbial metabolic pathways among groups based on alterations in the composition of intestinal flora (Fig. 6). The investigation identified the top 10 metabolic pathways with the greatest proportion and P-value < 0.05. The findings demonstrated that probiotic L9 group exhibited a remarkable rise in the relative abundance of fatty acid metabolism, glycerophospholipid metabolism, and propanoate metabolism (P < 0.05, Fig. 6B). Conversely, the A6 group demonstrated an exceptionally significant increase in the relative abundances of glycolysis/gluconeogenesis and fatty acid metabolism (P < 0.01, Fig. 6B).

3.7 L9 and A6 treatment changed metabolites in serum

PCA analysis of LC-MS data from serum samples showed a distinct distribution of metabolite profile after A6 and L9 intervention (Fig. 7A). Similarity analysis also showed that there were significant differences in metabolite composition between the probiotic groups and the AD model group (P < 0.05).

In order to explore the effect of probiotic intervention on serum metabolites in AD mice, VIP > 1 and P < 0.05 were used as the screening criteria for differential metabolites, and 10 and 9 differential metabolites were identified in probiotic L9 and A6 groups, respectively. Meanwhile, we draw the volcano map based on the Fc values and t-test results and conducted hierarchical clustering through the heatmap (Figs. 7B and C). The results showed that 4-vinylphenol sulfate, pantothenic acid, *n*-methylvaline, dodecylbenzenesulfonic acid and *L*-alloisoleucine were significantly up-regulated, while citric acid, 8,11-eicosadiynoic acid, linoleic acid, palmitic acid and phosphatidylcholine (PC) (16:0/16:0) were significantly down-regulated in probiotic L9 group. In A6 group, 4-vinylphenol sulfate, *p*-tolyl sulfate, pyrocatechol sulfate, phosphatidylethanolamine (PE, 22:5/P-16:0),

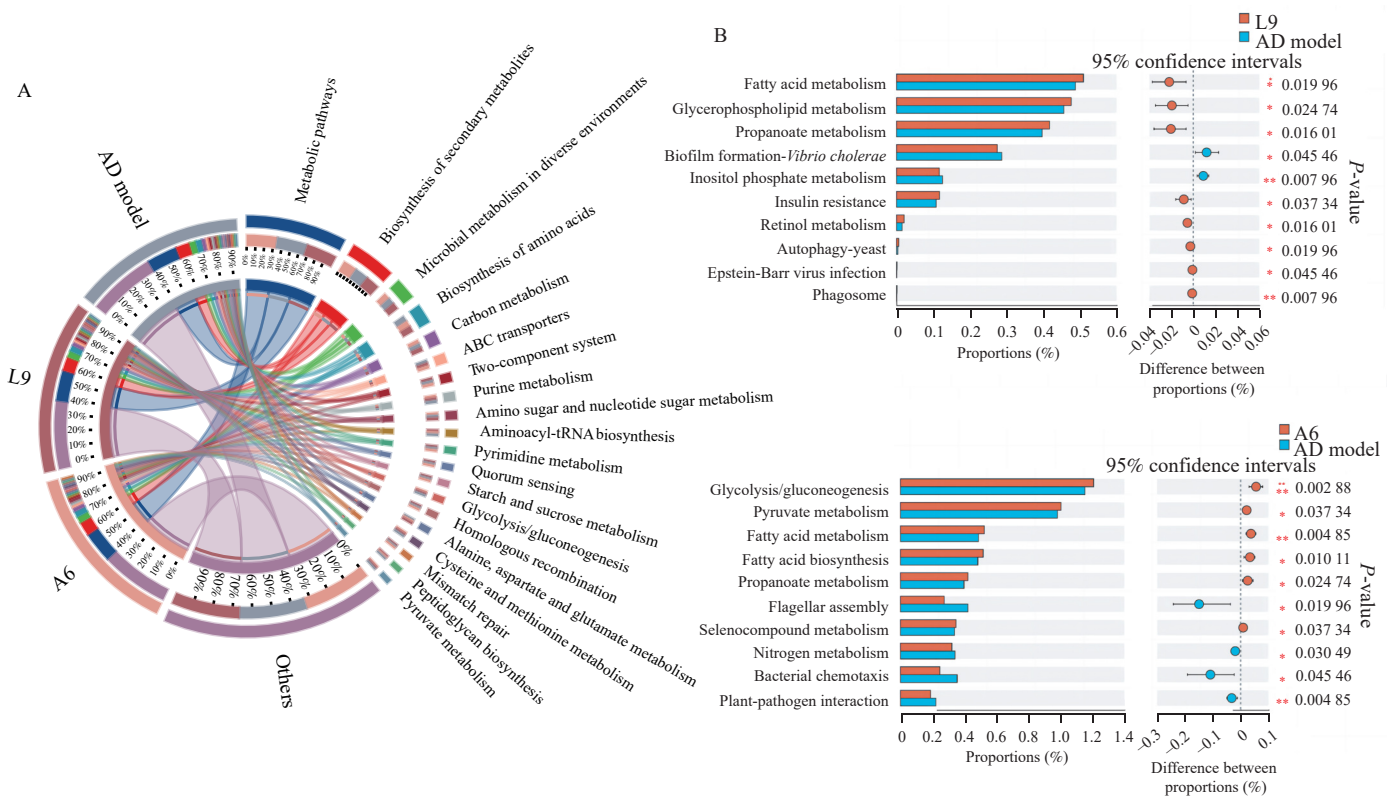

Fig. 6 Effects of L9 or A6 treatment on metabolic functional prediction of altered gut microbiota in AD-model mice (n = 10/group). (A) Circos diagram shows the abundance correspondence between samples and metabolic functions. (B) Differential KEGG pathways between L9/A6 and AD model group were predicted using PICRUSt analysis (*P < 0.05, **P < 0.01).

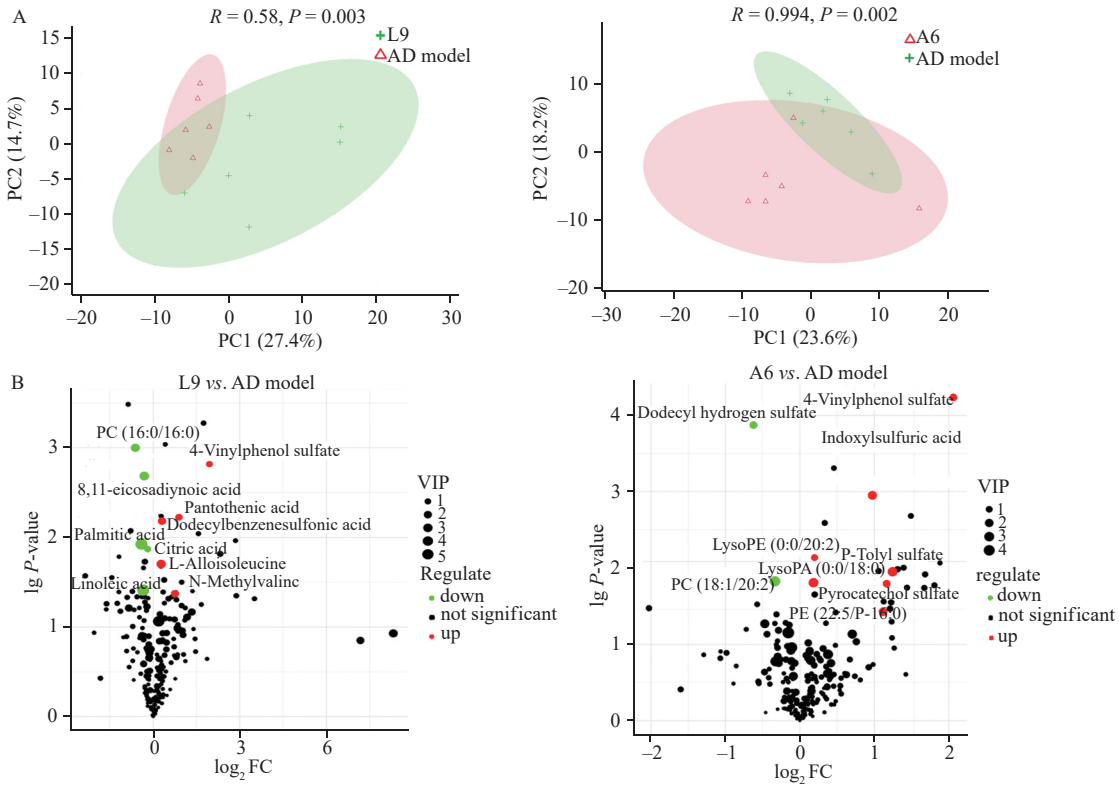

Fig. 7 Effects of L9 or A6 administration on serum metabolites in AD-model mice (n = 6/group). (A) Principal components analysis (PCA) scores of serum metabolites in mice between L9/A6 and AD model group. (B) Volcano diagrams of differential metabolites in L9, A6 and AD model group. The red dots in the figure represent up-regluated metabolites, and the black dots represent no significant difference while the green dots represent down-regluated metabolites (VIP > 1, P < 0.05). (C) Heatmap of the significantly expressed metabolites in metabolism related pathways between L9/A6 and AD model groups.

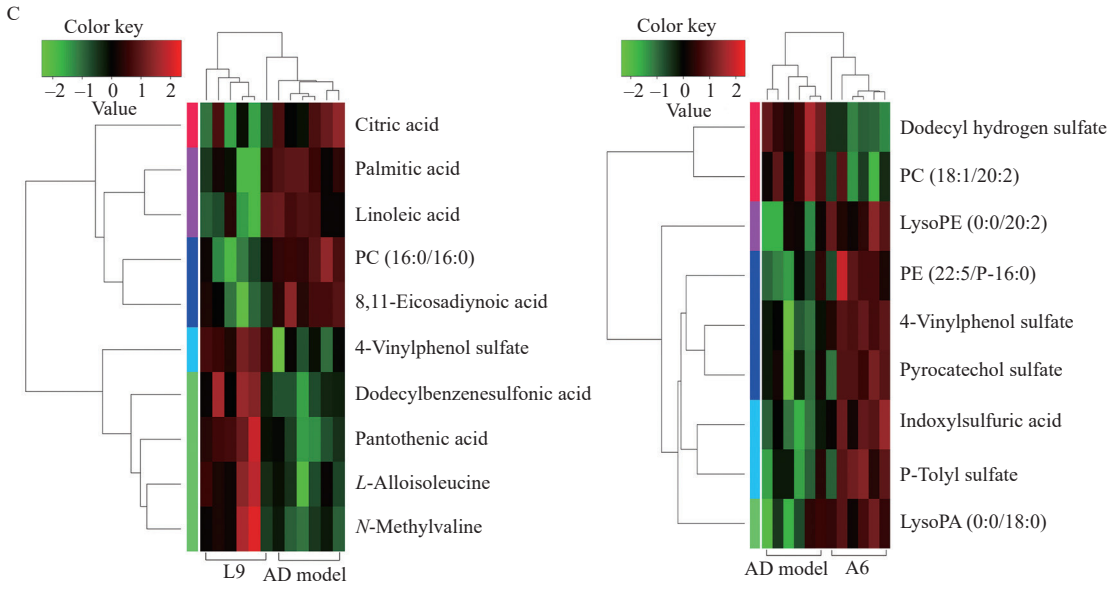

Fig. 7 (*Continued*)

indoxylsulfuric acid, lysoPE (0:0/20:2) and lysoPA (0:0/18:0) were significantly up-regulated, while PC (18:1) and dodecyl hydrogen sulfate were significantly down-regulated. In general, significant changes of differential metabolites in serum were observed after probiotics intervention, which maybe closely related to the mechanism of probiotics improving AD.

3.8 Spearman correlation analysis between serum metabolites and gut microbiota

A Spearman correlation analysis was performed to access correlation between differential serum metabolites and top 30 microbiological genus in mice (Fig. 8). The correlation analysis of AD and L9 groups showed

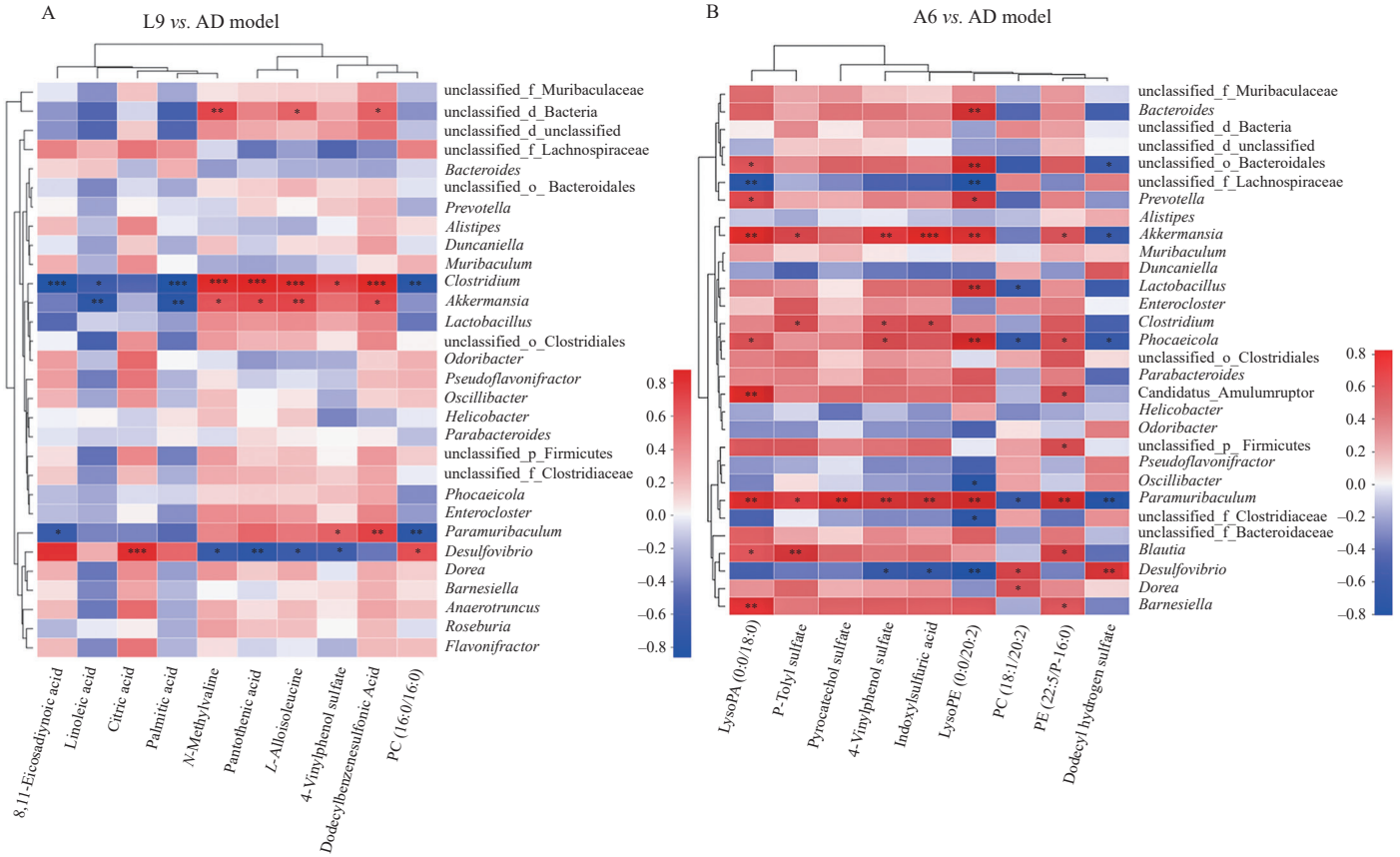

Fig. 8 Spearman correlation of serum differential metabolites and gut microbiota ($n = 6$/group). (A) Correlation between L9 and AD model group. (B) Correlation between A6 and AD model group. Red for positive correlation, and blue for negative correlation (*$P < 0.05$, **$P < 0.01$, ***$P < 0.001$).

that the abundance of *Clostridium*, *Akkemansia*, *Paramuribaculum* and *Desulfovibrio* were highly correlated with the abundance of differential metabolites. *Desulfovibrio*, which was enriched in AD group, was positively correlated with the abundance of citric acid, PC (16:0/16:0), palmitic acid and 8,11-eicosadiynoic acid. By contrast, *Clostridium*, *Akkemansia* and *Paramuribaculum* were negatively correlated with the intensity of the above 4 compounds, and showed a positive correlation with the intensity of *n*-methylvaline, pantothenic acid, 4-vinylphenol sulfate, *L*-alloisoleucine and dodecylbenzenesulfonic acid.

The correlation analysis of AD and A6 groups showed that the abundance of *Akkemansia*, *Clostridium Phocaeiola*, *Paramuribaculum* and *Desulfovibrio* were highly correlated with the abundance of differential metabolites. *Desulfovibrio* was positively correlated with the abundance of dodecyl hydrogen sulfate and PC (18:1/20:2). *Clostridium*, *Akkemansia Phocaeiola* and *Paramuribaculum* were negatively correlated with the intensity of dodecyl hydrogen sulfate and PC (18:1/20:2), and showed a positive correlation with the intensity of lysoPA (0:0/18:0), p-tolyl sulfate, pyrocatechol sulfate, 4-vinylphenol sulfate, indoxylsulfuric acid, lysoPE (0:0/20:2) and PE (22:5/P-16:0).

4. Discussion

Accumulating evidence has indicated that probiotics exert a significant influence on the prevention and treatment of AD through their regulation of the microbial-gut-brain axis[30], thereby impacting host brain function and behavior. However, further extensive research is required to fully comprehend the precise mechanism underlying the therapeutic effects of probiotics in AD. In this study, we established an AD animal model and observed that the administration of probiotics L9 and A6 effectively ameliorated the impairment of learning and memory function in AD mice. Additionally, L9 and A6 intervention regulated Tau phosphorylation by balancing activity of GSK-3β and PP2A kinases, and L9 and A6 inhibited Aβ deposition in the hippocampus of mice. More importantly, the probiotic L9 and A6 intervention taxonomic composition of the intestinal microbiome, and reduced the abundance of pathogenic bacterial genera *Desulfovibrio*, increased the abundance of beneficial genera *Clostridium* and *Paramuribaculum*. The fatty acids metabolism and biosynthesis of gut microbiome were also enhanced. Serum metabolomics also showed significant changes in blood levels of lipid-related metabolites, which may directly or indirectly mitigate the pathogenesis of AD. These results provided new evidence for a mechanism by which probiotics alleviate AD through the gut-brain axis.

In AD research, the main focus is on inhibiting the accumulation of Aβ and phosphorylation of Tau in the brain, as these abnormal processes are widely acknowledged as the primary causes of cognitive decline associated with the disease[31]. The hippocampus CA1 region, as an important brain region responsible for learning and memory in the hippocampus, is highly susceptible to the effects of Aβ and Tau proteins in AD patients[32]. In the current study, HE staining revealed that L9 and A6 could reduce cell edema and abnormal changes in CA1 region of AD mice.

The Tau protein plays a critical role in maintaining the stability of the neuron cytoskeleton and facilitating proper neuronal function[33]. In individuals with AD, the concentration of Tau in the brain is elevated compared to that of healthy individuals. This increased concentration leads to the hyperphosphorylation of Tau protein, resulting in the formation of a double helix structure that impairs its ability to effectively bind to tubulin. Consequently, the loss of microtubule stability occurs, leading to the aggregation of NFTs and subsequent damage to tubulin structures in the brain of AD patients. Ultimately, this pathological process contributes to the decline in normal cognitive function observed in individuals with AD[34-36]. Research has demonstrated that Tau possesses multiple phosphorylation sites with distinct functions, and in the cerebrospinal fluid of individuals with AD, Tau is extensively phosphorylated at the Ser396 and Ser404 sites[37]. Present WB findings indicate that the probiotics L9 and A6 significantly diminish the expression of phosphorylated Tau protein at the Ser396 and Ser404 sites in the hippocampus of AD mice.

Furthermore, the phosphorylation of Tau is regulated by various protein kinases and phosphatases, with GSK-3β kinase and PP2A phosphatase playing a prominent role in the process of hyperphosphorylation[38]. Yin et al.[39] have demonstrated that inhibiting GSK-3β can improve Tau hyperphosphorylation in the hippocampus of rats with AD. The activation of PP2A has been shown to attenuate Tau hyperphosphorylation and enhance learning and memory[40]. The balance between PP2A and GSK-3β levels is considered crucial for the regulation of Tau phosphorylation[41]. Our findings indicate an increase in GSK-3β and a decrease in PP2A in AD patients, which aligns with previous research[42]. Probiotics L9 and A6 have the potential to directly modulate the activities of PP2A and GSK-3β enzymes, thereby influencing Tau phosphorylation and improving cognition and learning in mice with AD.

Aβ is obtained from amyloid precursor protein by β and γ hydrolase decomposition, mainly including $A\beta_{1-40}$ and $A\beta_{1-42}$[43]. The Aβ deposition in the cell matrix to form plaques was reported to promote Tau phosphorylation, including activation of GSK-3β[44]. Existing studies have shown that the imbalance of Aβ production and clearance can lead to neuroinflammation, then activated microglia and produced AD-related inflammatory factors, which is also an important mechanism in the pathogenesis of AD[45]. Currently, *Bifidobacterium lactis* Pro-M8 inhibited Aβ plaque formation to prevent the occurrence of AD[46]. In our study, the administration of probiotics L9 and A6 also reduced the deposition of $A\beta_{1-40}$ and $A\beta_{1-42}$ proteins in the CA1 region of the hippocampus. Based on above results, we speculated that the intake of probiotics reduced Aβ deposition in the hippocampus, which in turn reduced activation of PP2A and GSK-3β and the phosphorylation of Tau proteins. The inhibition of phosphorylation of Tau conversely contributed to alleviate the deposition of Aβ.

The beneficial effect of probiotics on the central nervous system or AD symptoms is closely related to their ability to improve intestinal flora. Dysbiosis of the intestinal flora has also been recognized as an important trigger in the pathogenesis of AD[47]. The intestinal microbial population of AD mice is usually dominated by Bacteroidetes, Proteobacteria and Firmicutes in the phylum level[48]. In the current study, some structural changes in the intestinal flora of mice in the AD model group were also observed. LEfSe analysis shows that *Bacteroides*, *Desulfovibrio* and *Oscillibacter* are distinctly enriched in the AD group. Chen et al.[49] reported that *Bacteroides* mediating pro-inflammatory PUFA regulated microglia activation in the brain of AD mice, and indirectly enhanced the pathology and cognitive impairment of AD mice. *Desulfovibrio*, as an inflammatory-related bacteria, has been proven to be associated with the pathological developments of AD and other central nervous system diseases[50]. A previous study demonstrated that

the abundance of *Oscillibacter* increased with increased carcinogenesis-induced inflammation and obesity-related inflammation, and its increase may be associated with abnormal intestinal permeability[51]. L9 and A6 intervention decreased the relative abundance of *Bacteroides*, *Desulfovibrio* and *Oscillibacter*. These results suggest that the abundance of opportunistic pathogens associated with inflammation can be reduced with the ingestion of L9 and A6.

Based on the microbiota results, *Clostridium* was the discriminative species in the L9 treatment group. As *Clostridium* has a strong metabolism of fatty acids and glycerophospholipids, the rise of this species was able to increase the catabolism of fatty acids and glycerophospholipids by the flora[52]. Correlation analysis showed that *Clostridium* was significantly negatively correlated with serum levels of the PC, linoleic acid, and palmitic acid. The concentration of PC, as an important glycerophospholipid, was elevated in the cerebrospinal fluid of AD patients and affected abnormal $A\beta_{1\text{-}42}$ values, possibly symboling neurodegeneration and loss of membrane function in early cognitive impairment[53]. There was significant accumulation of FFAs in the hippocampus and cortex of AD mice, including palmitic acid and linoleic acid, both of which are involved in fatty acid metabolism[54]. N-6 polyunsaturated fatty acid linoleic acid promotes inflammation in the hippocampus. Excessive linoleic acid induced the polymerization of Aβ and Tau[55-56]. The intervention of L9 may indirectly reduce the production of inflammation-related arachidonic acid, and minimize AD-associated neuroinflammation by regulating the metabolism of linoleic acid. Palmitic acid leads to a pro-inflammatory microenvironment that damage the integrity of the blood-brain barrier. Palmitic acid could easily cross the barrier into the brain and the accumulation of PA triggers lipo-toxicity which induces Tau hyperphosphorylation and Aβ deposition[57-58]. Therefore, the intervention of L9 might increase the abundance of *Clostridium* to reduce these potentially harmful metabolites in favor of reducing neuroinflammation and improving AD symptoms.

In the A6-treated group, *Paramuribaculum* was discriminative species. Correlation analyses (Fig. 8) showed that *Paramuribaculum* was significantly positively correlated with the increase of lysophosphatidic acid (LysoPA), lysophosphatidylethanolamine (LysoPE) and glycerophospholipid PE. Lysophospholipids are generated by the action of phospholipase and are used to regenerate phospholipids in the remodeling pathway[59]. Elevation of the lysophospholipid levels could help to alleviate nerve cell damage and promote nerve cell proliferation[60]. LysoPA has been proven to be an important regulatory factor in the development of the cerebral cortex and neurogenesis, as it can regulate the development of the nervous system by binding to a variety of lysoPA receptors[61]. Metabolic dysfunction of lysoPA can lead to abnormal deposition of Aβ, formation of NFT, and neuroinflammation, ultimately resulting in neuronal death[62]. Furthermore, LysoPE has been widely reported to be decreased in patients with AD[63]. LysoPE is involved in stimulating synaptic growth in the brain and may have potential physiological effects on brain development[64]. Compared to PC, another glycerophospholipid PE has been shown to reverse amyloid-related cognitive impairment in a rat model of AD, and the level of PE were found to decline in serum in AD patients[65]. In our study, A6 treatment influenced the relative abundance of *Paramuribaculum* and also increased the levels of lysoPA, lysoPE and PE (22:5/16:0). Although we speculated that *Paramuribaculum* may act as a beneficial bacterium in the mammalian gut microbiota, potentially associated with its ability to synthesize and metabolize fatty acids, further research is needed to determine its therapeutic effects on AD.

Until now, the effect of microbiota and metabolites on the improvement of AD is very limited, and there are even greater possibilities to reduce the occurrence of AD by changing the composition of intestinal microorganisms and serum metabolites. In addition, this study conducted animal experiments using male mice and found that gender differences also have a certain impact on the gut microbiota[66]. It was observed that there is a bidirectional influence between sex hormone levels and gut microbiota[67]. Furthermore, females are more susceptible to depression and Alzheimer's disease during certain special periods due to changes in sex hormone levels compared to males[68]. Therefore, considering the gender differences in gut microbiota and the sensitivity of females to diseases, female mice should also be included in future studies on the microbiota-gut-brain axis.

5. Conclusion

In conclusion, oral administration of probiotics L9 and A6 effectively improved cognitive dysfunction and inhibited Aβ aggregation and Tau hyperphosphorylation in AD mice. The inhibitory effects on Tau phosphorylation and the Aβ deposition maybe mediated *via* GSK-3β and PP2A kinases. Meanwhile, by metagenomic sequencing, we found the probiotic L9 and A6 intervention altered taxonomic composition of the intestinal microbiome, and reduced the abundance of pathogenic genera *Desulfovibrio*, increased the abundance of beneficial genera *Clostridium* and *Paramuribaculum*. The fatty acids metabolism and biosynthesis of gut microbiome were also enhanced. Serum untargeted metabolomics also showed significant changes in blood levels of lipid-related metabolites, which may alleviate the pathogenesis of AD. These results revealed a mitigating role for probiotic L9 and A6 in AD prevention and offer new insights into AD prevention *via* gut-brain connection.

Conflict of interest

The authors declared that there is no conflict of interest.

Acknowledgements

This research was funded by the National Key R&D Program of China (2023YFF1104501), R&D Program of Beijing Municipal Education Commission (23JF0006), National Natural Science Foundation of China (31601443 and 32101938). We thank the Figdraw tool (www.figdraw.com) for figure services.

Appendix A. Supplementary information

Supplementary data associated with this article can be found, in the online version, at http://doi.org/10.26599/FSHW.2024.9250340.

References

[1] J. Doroszkiewicz, P. Mroczko, A.Kulczynska-Przybik, Inflammation in the CNS: understanding various aspects of the pathogenesis of Alzheimer's disease, Curr. Alzheimer Res. 19 (2022) 16-31. http://doi.org/10.2174/1567205018666211202143935.

[2] X.X. Zhang, Y. Tian, Z.T. Wang, et al., The epidemiology of Alzheimer's disease modifiable risk factors and prevention, J. Prev. Alzheimer's Dis. 8 (2021) 313-321. http://doi.org/10.14283/jpad.2021.15.

[3] M. Liu, P. Zhong, Modulating the gut microbiota as a therapeutic intervention for Alzheimer's disease, Indian J. Microbiol. 62 (2022) 494-504. http://doi.org/10.1007/s12088-022-01025-w.

[4] U. Chockanathan, K. Padmanabhan, From synapses to circuits and back: bridging levels of understanding in animal models of Alzheimer's disease, Eur. J. Neurosci. 56 (2022) 5564-5586. http://doi.org/10.1111/ejn.15636.

[5] D.K. Kim, J. Park, D. Han, et al., Molecular and functional signatures in a novel Alzheimer's disease mouse model assessed by quantitative proteomics, Mol. Neurodegener. 13 (2018) 2. http://doi.org/10.1186/s13024-017-0234-4.

[6] J. Miao, R. Shi, L. Li, et al., Pathological Tau from Alzheimer's brain induces site-specific hyperphosphorylation and SDS- and reducing agent-resistant aggregation of Tau *in vivo*, Front. Aging Neurosci. 11 (2019) 34. http://doi.org/10.3389/fnagi.2019.00034.

[7] G. Taleski, E. Sontag, Protein phosphatase 2A and Tau: an orchestrated 'Pas de Deux', FEBS Lett 592 (2018) 1079-1095. http://doi.org/10.1002/1873-3468.12907.

[8] O. Seira, J.A. Del Rio, Glycogen synthase kinase 3 beta (GSK3beta) at the tip of neuronal development and regeneration, Mol. Neurobiol. 49 (2014) 931-944. http://doi.org/10.1007/s12035-013-8571-y.

[9] M. Jin, N. Shepardson, T. Yang, et al., Soluble amyloid beta-protein dimers isolated from Alzheimer cortex directly induce Tau hyperphosphorylation and neuritic degeneration, PNAS 108 (2011) 5819-5824. http://doi.org/10.1073/pnas.1017033108.

[10] Y.H. Escobar, D. O'Piela, L.E. Wold, et al., Influence of the microbiota-gut-brain axis on cognition in Alzheimer's disease, J. Alzheimers's Dis. 87 (2022) 17-31. http://doi.org/10.3233/JAD-215290.

[11] S.R. Zhong, Q. Kuang, F. Zhang, et al., Functional roles of the microbiota-gut-brain axis in Alzheimer's disease: implications of gut microbiota-targeted therapy, Transl. Neurosci. 12 (2021) 581-600. http://doi.org/10.1515/tnsci-2020-0206.

[12] E.M.M. Quigley, Microbiota-brain-gut axis and neurodegenerative diseases, Curr. Neurol Neurosci Rep. 17 (2017) 94. http://doi.org/10.1007/s11910-017-0802-6.

[13] E. R. Murray, M. Kemp, T. T. Nguyen, The microbiota-gut-brain axis in Alzheimer's disease: a review of taxonomic alterations and potential avenues for interventions, Arch. Clin. Neuropsychol. 37 (2022) 595-607. http://doi.org/10.1093/arclin/acac008.

[14] A. Cattaneo, N. Cattane, S. Galluzzi, et al., Association of brain amyloidosis with pro-inflammatory gut bacterial taxa and peripheral inflammation markers in cognitively impaired elderly, Neurobiol. Aging 49 (2017) 60-68. http://doi.org/10.1016/j.neurobiolaging.2016.08.019.

[15] B.L. Sun, W.W. Li, J. Wang, et al., Gut microbiota alteration and its time course in a tauopathy mouse model, J. Alzheimers's Dis. 70 (2019) 399-412. http://doi.org/10.3233/JAD-181220.

[16] X.L. Wang, J. Zeng, Y. Yang, et al., *Helicobacter pylori* filtrate induces Alzheimer-like Tau hyperphosphorylation by activating glycogen synthase kinase-3β, J. Alzheimers's Dis. 43 (2015) 153-165. http://doi. org/10.3233/JAD-140198.

[17] C. Mancuso, R. Santangelo, Alzheimer's disease and gut microbiota modifications: the long way between preclinical studies and clinical evidence, Pharmacol. Res. 129 (2018) 329-336. http://doi.org/10.1016/j.phrs.2017.12.009.

[18] Z. Ling, M. Zhu, X. Yan, et al., Structural and functional dysbiosis of fecal microbiota in Chinese patients with Alzheimer's disease, Front. Cell. Dev. Biol. 8 (2020) 634069. http://doi.org/10.3389/fcell.2020.634069.

[19] Y. Kobayashi, H. Sugahara, K. Shimada, et al., Therapeutic potential of *Bifidobacterium breve* strain A1 for preventing cognitive impairment in Alzheimer's disease, Sci. Rep. 7 (2017) 13510. http://doi.org/10.1038/s41598-017-13368-2.

[20] X. Song, Z. Zhao, Y. Zhao, et al., *Lactobacillus plantarum* DP189 prevents cognitive dysfunction in *D*-galactose/$AlCl_3$ induced mouse model of Alzheimer's disease *via* modulating gut microbiota and PI3K/Akt/GSK-3β signaling pathway, Nutr. Neurosci, 25 (2022) 2588-2600. http://doi. org/10.1080/1028415X.2021.1991556.

[21] M. Abdelhamid, C. Zhou, C.G. Jung, et al., Probiotic *Bifidobacterium breve* MCC1274 mitigates Alzheimer's disease-related pathologies in wild-type mice, Nutrients 14 (2022) 2543. http://doi.org/10.3390/nu14122543.

[22] H.J. Lee, K.E. Lee, J.K. Kim, et al., Suppression of gut dysbiosis by *Bifidobacterium longum* alleviates cognitive decline in 5XFAD transgenic and aged mice, Sci. Rep. 9 (2019) 11814. http://doi.org/10.1038/s41598-019-48342-7.

[23] Y. Meng, X. Qiu, Z. Tang, et al., *Lactobacillus paracasei* L9 affects disease progression in experimental autoimmune neuritis by regulating intestinal flora structure and arginine metabolism, J. Neuroinflammation. 20 (2023) 122. http://doi.org/10.1186/s12974-023-02808-8.

[24] E. Sun, L. Zhao, F. Ren, et al., Complete genome sequence of *Bifidobacterium animalis* subsp. lactis A6, a probiotic strain with high acid resistance ability, J. Biotechnol. 200 (2015) 8-9. http://doi.org/10.1016/j.jbiotec.2015.02.016.

[25] F. Wu, G. Wuri, B. Fang, et al., Alleviative mechanism and effect of *Bifidobacterium animalis* A6 on dextran sodium sulfate-induced ulcerative colitis in mice, Food Sci. Nutr. 11 (2022) 892-902. http://doi.org/10.1002/fsn3.3124.

[26] C. Tan, Y. Liu, H. Zhang, et al., Neuroprotective effects of probiotic-supplemented diet on cognitive behavior of 3xTg-AD Mice, J. Healthc. Eng. 2022 (2022) 4602428. http://doi.org/10.1155/2022/4602428.36.

[27] X. Song, Z. Zhao, Y. Zhao, et al., Protective effects of *Bacillus coagulans* JA845 against *D*-Galactose/AlCl3-Induced cognitive decline, oxidative stress and neuroinflammation, J. Microbiol. Biotechnol. 32 (2022) 212-219. http://doi.org/10.4014/jmb.2111.11031.

[28] F. Wu, B. Fang, G. Wuri, et al., Metagenomic analysis reveals a mitigating role for *Lactobacillus paracasei* and *Bifidobacterium animalis* in experimental periodontitis, Nutrients 14 (2022) 2125. http://doi.org/10.3390/nu14102125.

[29] X. Zhang, X. Liu, J. Yang, et al., Quantitative profiling of bile acids in feces of humans and rodents by ultra-high-performance liquid chromatography-quadrupole time-of-flight mass spectrometry, Metabolites 12 (2022) 633. http://doi.org/10.3390/metabo12070633.

[30] L.F. Iannone, A. Preda, H.M. Blottiere, et al., Microbiota-gut brain axis involvement in neuropsychiatric disorders, Expert Rev. Neurother. 19 (2019) 1037-1050. http://doi.org/10.1080/14737175.2019.1638763.

[31] Y. Ju, K.Y. Tam, Pathological mechanisms and therapeutic strategies for Alzheimer's disease, Neural Regen Res. 17 (2022) 543-549. http://doi.org/10.4103/1673-5374.320970.

[32] D. Ji, X. Wu, D. Li, et al., Protective effects of chondroitin sulphate nano-selenium on a mouse model of Alzheimer's disease, Int. J. Biol. Macromol. 154 (2020) 233-245. http://doi.org/10.1016/j.ijbiomac.2020.03.079.

[33] S. Wegmann, J. Biernat, E. Mandelkow, A current view on Tau protein phosphorylation in Alzheimer's disease, Curr. Opin. Neurobiol. 69 (2021) 131-138. http://doi.org/10.1016/j.conb.2021.03.003.

[34] A.R. Duan, E.M. Jonasson, E.O. Alberico, et al., Interactions between Tau and different conformations of tubulin: implications for Tau function and mechanism, J. Mol. Biol. 429 (2017) 1424-1438. http://doi.org/10.1016/j.jmb.2017.03.018.

[35] F.P. Chong, K.Y. Ng, R.Y. Koh, et al., Tau proteins and tauopathies in Alzheimer's disease. Cell Mol. Neurobiol. 38 (2018) 965-980. http://doi.org/10.1007/s10571-017-0574-1.

[36] S. Mondragon-Rodriguez, G. Basurto-Islas, I. Santa-Maria, et al., Cleavage and conformational changes of Tau protein follow phosphorylation during Alzheimer's disease, Int. J. Exp. Pathol. 89 (2008) 81-90. http://doi.org/10.1111/j.1365-2613.2007.00568.x.

[37] Y. Xia, S. Prokop, B.I. Giasson, "Don't Phos Over Tau": recent developments in clinical biomarkers and therapies targeting Tau phosphorylation in Alzheimer's disease and other tauopathies, Mol. Neurodegener. 16 (2021) 37. http://doi.org/10.1186/s13024-021-00460-5.

[38] J.Z. Wang, I. Grundke-Iqbal, K. Iqbal, Kinases and phosphatases and Tau sites involved in Alzheimer neurofibrillary degeneration, Eur. J. Neurosci. 25 (2007) 59-68. http://doi.org/10.1111/j.1460-9568.2006.05226.x.

[39] J. Yin, Y.H. Liu, Y.F. Xu, et al., Melatonin arrests peroxynitrite-induced Tau hyperphosphorylation and the overactivation of protein kinases in rat brain, J. Pineal. Res. 41 (2006) 124-129. http://doi. org/10.1111/j. 1600-079X.2006.00343.x.

[40] Y. Y. Yin, H. Liu, X.B. Cong, et al., Acetyl-*L*-carnitine attenuates okadaic acid induced Tau hyperphosphorylation and spatial memory impairment in rats, J. Alzheimers's Dis. 19 (2010) 735-746. http://doi.org/10.3233/JAD-2010-1272.

[41] Y. Zhang, X. Fan, Z. Su, et al., Pretreatment with metformin prevents microcystin-LR-induced Tau hyperphosphorylation *via* mTOR-dependent PP2A and GSK-3β activation, Environ. Toxicol. 36 (2021) 2414-2425. http://doi.org/10.1002/tox.23354.

[42] W. Wei, Y.H. Liu, C.E. Zhang, et al., Folate/vitamin-B12 prevents chronic hyperhomocysteinemia-induced Tau hyperphosphorylation and memory deficits in aged rats, J. Alzheimers's Dis. 27 (2011) 639-650. http://doi.org/10.3233/JAD-2011-110770.

[43] G.F. Chen, T.H. Xu, Y. Yan, et al., Amyloid beta: structure, biology and structure-based therapeutic development, Acta Pharmacol. Sin. 38 (2017) 1205-1235. http://doi.org/10.1038/aps.2017.28.

[44] S.H. Koh, M.Y. Noh, S. H. Kim, Amyloid-beta-induced neurotoxicity is reduced by inhibition of glycogen synthase kinase-3, Brain Res. 1188 (2008) 254-262. http://doi.org/10.1016/j.brainres.2007.10.064.

[45] P. d'Errico, S. Ziegler-Waldkirch, V. Aires, et al., Microglia contribute to the propagation of Aβ into unaffected brain tissue, Nat. Neurosci. 25 (2021) 20-25. http://doi:10.1038/s41593-021-00951-0.

[46] J. Cao, W. K. Amakye, C. Qi, et al., *Bifidobacterium Lactis* probio-M8 regulates gut microbiota to alleviate Alzheimer's disease in the APP/PS1 mouse model, Eur. J. Nutr. 60 (2021) 3757-3769. http://doi.org/10.1007/s00394-021-02543-x.

[47] S. Westfall, N. Lomis, I. Kahouli, et al., Microbiome, probiotics and neurodegenerative diseases: deciphering the gut brain axis, Cell. Mol. Life Sci. 74 (2017) 3769-3787. http://doi.org/10.1007/s00018-017-2550-9.

[48] L. Zhang, Y. Wang, X. Xiayu, et al., Altered gut microbiota in a mouse model of Alzheimer's disease, J. Alzheimers's Dis. 60 (2017) 1241-1257. http://doi.org/10.3233/JAD-170020.

[49] C. Chen, J. Liao, Y. Xia, et al., Gut microbiota regulate Alzheimer's disease pathologies and cognitive disorders *via* PUFA-associated neuroinflammation, Gut 71 (2022) 2233-2252. http://doi.org/10.1136/gutjnl-2021-326269.

[50] H. Zhou, J. Tai, H. Xu, et al., Xanthoceraside could ameliorate Alzheimer's disease symptoms of rats by affecting the gut microbiota composition and modulating the endogenous metabolite levels, Front. Pharmacol. 10 (2019) 1035. http://doi.org/10.3389/fphar.2019.01035.

[51] K. Sakurai, T. Toshimitsu, E. Okada, et al., Effects of *Lactiplantibacillus plantarum* OLL2712 on memory function in older adults with declining memory: a randomized placebo-controlled trial, Nutrients 14 (2022) 4300. http://doi.org/10.3390/nu14204300.

[52] J. Feng, J. Zhang, Y. Ma, et al., Renewable fatty acid ester production in *Clostridium*, Nat. Commun. 12 (2021) 4368. http://doi.org/10.1038/s41467-021-24038-3.

[53] M. Yi, C. Zhang, Z. Zhang, et al., Integrated metabolomic and lipidomic analysis reveals the neuroprotective mechanisms of bushen tiansui formula in an $A\beta_{1-42}$-induced rat model of Alzheimer's disease, Oxid. Med. Cell. Longev. 2020 (2020) 1-18. http://doi.org/10.1155/2020/5243453.

[54] J. Wang, R. Wei, G. Xie, et al., Peripheral serum metabolomic profiles inform central cognitive impairment, Sci. Rep. 10 (2020) 14059. http://doi.org/10.1038/s41598-020-70703-w.

[55] S.M. Alashmali, L. Lin, M.O. Trépanier, et al., The effects of *n*-6 polyunsaturated fatty acid deprivation on the inflammatory gene response to lipopolysaccharide in the mouse hippocampus, J. Neuroinflamm. 16 (2019) 237. http://doi.org/10.1186/s12974-019-1615-0.

[56] Z. Amtul, M. Uhrig, L. Wang, et al., Detrimental effects of arachidonic acid and its metabolites in cellular and mouse models of Alzheimer's disease: structural insight, Neurobiol. Aging 33 (2012) 831. e21-31. http://doi.org/10.1016/j.neurobiolaging.2011.07.014.

[57] D.J. Vesga-Jimenez, C. Martin, G.E. Barreto, Fatty acids: an insight into the pathogenesis of neurodegenerative diseases and therapeutic potential, Int. J. Mol. Sci. 23 (2022) 2577. http://doi.org/10.3390/ijms.

[58] K. Xie, Q. Qin, Z. Long, et al., High-throughput metabolomics for discovering potential biomarkers and identifying metabolic mechanisms in aging and Alzheimer's disease, Front. Cell Dev. Biol. 9 (2021) 602887. http://doi.org/10.3389/fcell.2021.602887.

[59] X. Zhang, W. Liu, J. Zan, et al., Untargeted lipidomics reveals progression of early Alzheimer's disease in APP/PS1 transgenic mice, Sci. Rep. 10 (2020) 14509. http://doi.org/10.1038/s41598-020-71510-z.

[60] S.T. Tan, T. Ramesh, X.R. Toh, et al., Emerging roles of lysophospholipids in health and disease, Prog. Lipid Res. 80 (2020) 101068. http://doi.org/10.1016/j.plipres.2020.101068.

[61] L.H.M. Geraldo, T.C.L.d.S. Spohr, R.F.d. Amaral, et al., Role of lysophosphatidic acid and its receptors in health and disease: novel therapeutic strategies, Signal Transduct Target Ther. 6 (2021) 45. http://doi.org/10.1038/s41392-020-00367-5.

[62] Y. Hao, M. Guo, Y. Feng, et al., Lysophospholipids and their G-coupled protein signaling in Alzheimer's disease: from physiological performance to pathological impairment, Front. Mol. Neurosci. 13 (2020) 58. http://doi.org/10.3389/fnmol.2020.00058.

[63] A. Strefeler, M. Jan, M. Quadroni, et al., Molecular insights into sex-specific metabolic alterations in Alzheimer's mouse brain using multi-omics approach, Alzheimer's Res. Ther. 15 (2023) 8. http://doi.org/10.1186/s13195-023-01162-4.

[64] M. Hachem, H. Nacir, Emerging role of phospholipids and lysophospholipids for improving brain docosahexaenoic acid as potential preventive and therapeutic strategies for neurological diseases, Int. J. Mol. Sci. 23 (2022) 3969. http://doi.org/10.3390/ijms23073969.

[65] H. Li, Y. Tan, X. Cheng, et al., Untargeted metabolomics analysis of the hippocampus and cerebral cortex identified the neuroprotective mechanisms of Bushen Tiansui formula in an Aβ25-35-induced rat model of Alzheimer's disease, Front. Pharmacol. 13 (2022) 990307. http://doi.org/10.3389/fphar.2022.990307.

[66] D. Cuervo-Zanatta, J. Garcia-Mena, C. Perez-Cruz, et al., Gut microbiota alterations and cognitive impairment are sexually dissociated in a transgenic mice model of Alzheimer's disease, J. Alzheimer's Dis. 82 (2021) S195-S214. http://doi.org/10.3233/jad-201367.

[67] S. He, H. Li, Z. Yu, et al., The gut microbiome and sex hormone-related diseases, Front. Microbiol. 12 (2021) 711137. http://doi.org/10.3389/fmicb.2021.711137.

[68] C. Barth, A. Crestol, A. de Lange, et al., Sex steroids and the female brain across the lifespan: insights into risk of depression and Alzheimer's disease. Lancet Diabetes Endo. 11 (2023) 926-941. http://doi.org/10.1016/s2213-8587(23)00224-3.